enkov cone. Specifically E and H are derivatives of potentials which drop abruptly from ∞ to 0 on the Cherenkov cone. In such a circumstance, the integral of Poynting's vector is indeterminate and must be evaluated by other means. For a particularly clear discussion of classical Cherenkov radiation see J. D. Jackson, *Classical Electrodynamics* (Wiley, New York, 1962) p. 495.

[20]An intriguing problem is posed by a TM going into an adverse magnetic field; i.e., one which tends to absorb energy from the particle. The TM cannot stop and retrace its path the way an ordinary particle can. H. K. Wimmel [Lett. Nuovo Cimento 2, 363 (1971)] argues that the tachyon will tunnel through the adverse field until it finds itself in a favorable field. Unfortunately, Wimmel's argument, which was made for electrically charged tachyons, cannot be directly transferred to the magnetic problem and in any event neglects Cherenkov radiation.

[21]Gammacell 220, Atomic Energy of Canada, Ltd., Ottawa, Canada.

[22]These rates are all about 20 times higher than the expected rate from accidental coincidences alone. The elevated rate persists when the source is removed and the phototubes optically shielded from one another. We have searched carefully for a malady in the recording system and have found none. Possibly the extra counts are caused by two correlated electrons in cosmic ray showers. These can interact directly in the photocathodes to liberate photoelectrons. (See Ref. 6 for a discussion of a similar problem.)

PHYSICAL REVIEW D VOLUME 6, NUMBER 7 1 OCTOBER 1972

Analysis of the Q in $K^-d \to K^-\pi^-\pi^+d$ and $K^-d \to K^-\pi^-\pi^+np_s$ at 7.3 GeV/c *

K. J. Anderson, A. D. Franklin, G. D. Godden, J. B. Kopelman, L. M. Libby, and T. H. Tan
University of Colorado, Boulder, Colorado 80302
(Received 22 November 1971)

Results from the study of reactions (1) $K^-d \to K^-\pi^-\pi^+d$ and (2) $K^-d \to K^-\pi^-\pi^+np_s$ at 7.3 GeV/c are presented. The interactions are dominated by the production of $K^*(890)$, $\rho(765)$, $Q(1200-1450)$, and $D^*(2200)$ in (1) and $\Delta^-(1236)$ in (2). Observation of $\rho(765)$ and its possible source as a misidentified $K^*(890)$ is discussed. Evidence is observed of splitting of the Q into two resonances with masses and widths (in MeV) $M_1 = 1228 \pm 21$, $\Gamma_1 = 111 \pm 33$, $M_2 = 1414 \pm 15$, and $\Gamma_2 = 89 \pm 24$. $L(1775)$ is observed in (1). An off-shell one-pion-exchange-model calculation is compared to (2). Cross sections and branching ratios of the Q resonances are estimated on the basis of the model.

INTRODUCTION

We present in this paper a study of K^-d interactions at 7.3 GeV/c. In particular, we are investigating the nature of the production of the $K\pi\pi$ enhancement in the Q region (1200–1450 MeV), as well as the structure and the decay properties of the Q. To date many pertinent questions concerning the Q enhancement remain unanswered and the subject continues to be an area of interest in strong-interaction physics.

The data on the Q available prior to May 1970 have been reviewed by Firestone at the 1970 Philadelphia Conference.[1] It was pointed out that while multi-Regge and Deck-type calculations have shown some success in fitting the data at lower momenta (below 7.3 GeV/c), similar success cannot be achieved when fitting the higher-energy data. In addition, results from most experiments indicate that the Q cannot be fitted by a single Breit-Wigner function. By fitting an accumulation of $K\pi\pi$ data from several experiments, Firestone found the Q to be consistent with a superposition of two peaks having masses and widths $M_1 = 1250 \pm 4$ MeV, $\Gamma_1 = 182 \pm 9$ MeV and $M_2 = 1400 \pm 6$ MeV, $\Gamma_2 = 220 \pm 14$ MeV. The results of our experiment appear to be in agreement with the above conjecture except for the widths of the two peaks which are narrower. The latter observation is in agreement with more recent experiments in K^+d at 9.0 GeV/c by Garfinkel *et al.* and in K^+p at 12 GeV/c by Davis *et al.*[2,3] Enhancements in the Q region have also been observed in nondiffractive experiments.[4-8] Mass and width values are again inconsistent, but the observations support the multiresonance interpretation of the diffractive data.

Uncertainty in a number of the other properties also remains. $K^*(890)\pi$ dominates the Q decay in the diffractive experiments while results on $K\rho(765)$ vary from 0% to 30%. No other modes have been observed. In the nondiffractive $\bar{p}p \to \bar{K}K\pi\pi$ annihilation experiment at rest, 75% $K\rho(765)$ is found for the enhancement observed at 1242 MeV.[7] From our analysis which is based

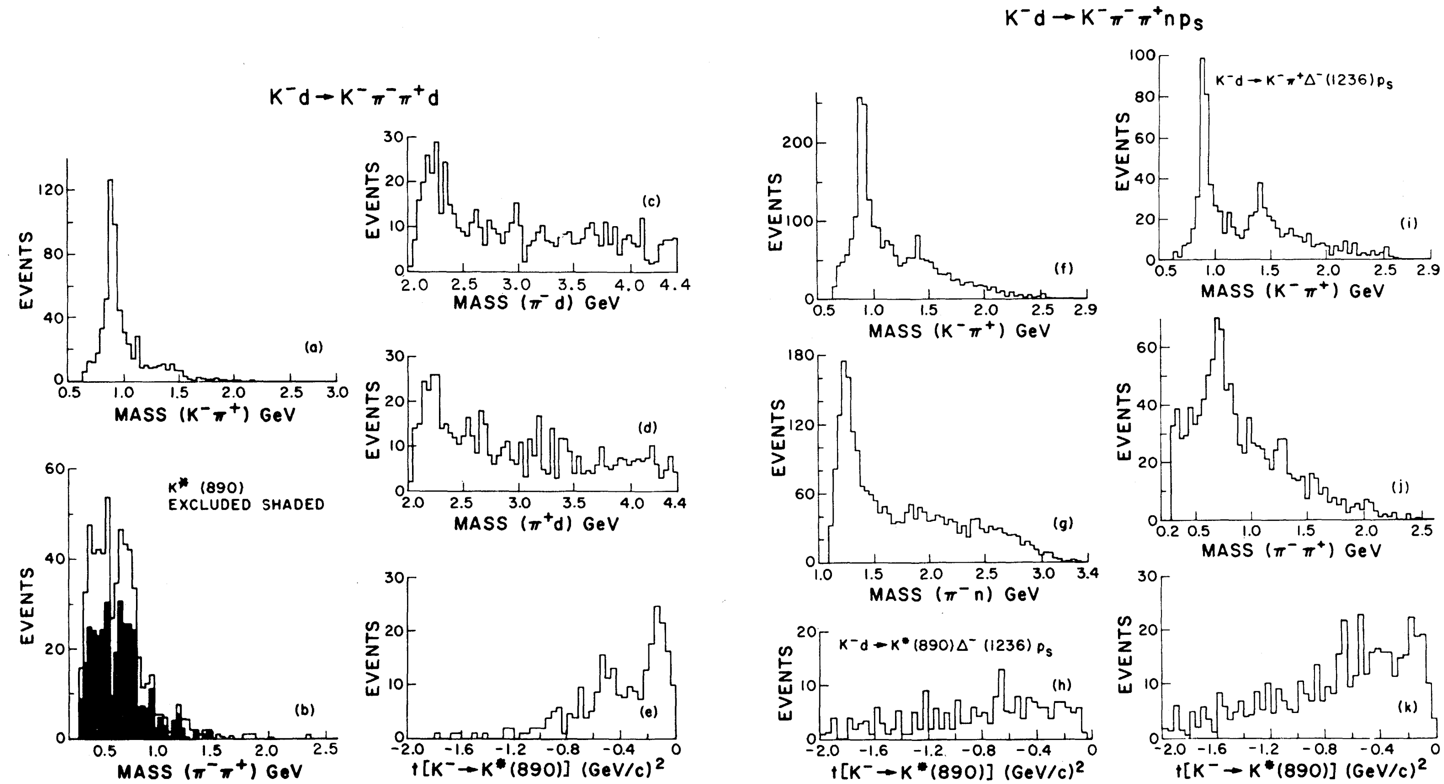

FIG. 1. From $K^-d \to K^-\pi^-\pi^+d$: (a) mass $(K^-\pi^+)$, (b) mass $(\pi^-\pi^+)$ with $K^*(890)$ removed shaded, (c) mass (π^-d), (d) mass (π^+d), and (e) $t(K^- \to K^*(890))$; and from $K^-d \to K^-\pi^-\pi^+np_s$: (f) mass $(K^-\pi^+)$, (g) mass (π^-n), (h) $t(K^- \to K^*(890))$ in $K^*(890)\Delta^-(1236)p_s$, (i) mass $(K^-\pi^+)$ in $K^-\pi^+\Delta^-(1236)p_s$, (j) mass $(\pi^-\pi^+)$ with $K^*(890)$ and $\Delta^-(1236)$excluded, and (k)$t(K \to K^*(890))$ when a $K^-\pi^-$ ambiguity occurred both fits were plotted weighted by $\frac{1}{2}$.

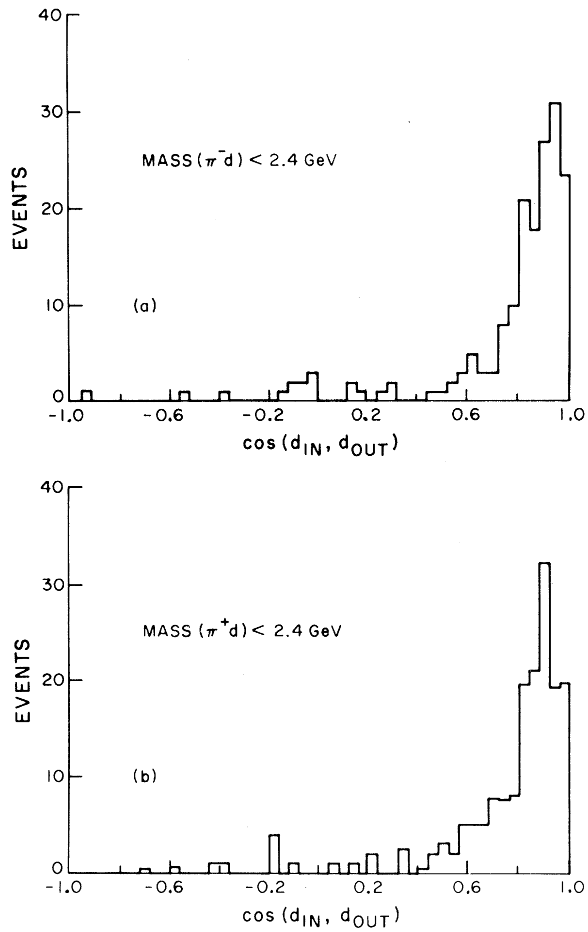

FIG. 2. (a) $\cos(d_{in}, d_{out})$ in the π^-d center-of-mass system with mass $(\pi^-d) < 2.4$ GeV. (b) $\cos(d_{in}, d_{out})$ in the π^+d center of mass with mass $(\pi^+d) < 2.4$ GeV for events in Fig. 1.

on a one-pion-exchange model, we estimate an upper limit of approximately 14% $K\rho(765)$ in our data.

A number of spin-parity analyses have been made on the Q. Most experiments favor 1^+ although 2^- has not been excluded.[2,3,9-12] Our statistics were not adequate for a meaningful determination although the entire Q region was found to be consistent with both the 1^+ and 2^- assignment. Coherent production off deuterium as in this experiment indicates that the Q has isospin $\frac{1}{2}$.

EXPERIMENTAL PROCEDURE

This experiment consisted of the analysis of three- and four-prong events from an exposure of the Brookhaven National Laboratory 80-in. deuterium-filled bubble chamber to the rf-separated K^--meson beam at 7.3 GeV/c. Events were processed by the kinematical fitting routines TVGP and SQUAW. In addition, a visual check of track ionization was made for all event fits. From these data the reactions

$$K^-d \to K^-\pi^-\pi^+d, \qquad (1)$$

$$K^-d \to K^-\pi^-\pi^+np_s \qquad (2)$$

were selected for further analysis. The sample consisted of 614 events of reaction (1) based on 110 000 frames of exposure and 2244 events of reaction (2) based on 52 000 frames of exposure. $K^-\pi^-\pi^+d$ events were selected using the characteristic proton-neutron momentum ratio and opening angle in the corresponding $K^-\pi^-\pi^+pn$ fits.[13] Reaction (2) consists of both three- and four-prong events. An upper momentum limit of 250 MeV/c has been applied to the visible proton spectator of the four-prong events. With this cutoff, the distribution of the cosine of the angle between the beam and the visible proton spectator in the laboratory frame is flat. Contamination from events of the type $K^-d \to \pi^-\pi^-\pi^+\Lambda p_s$ and $K^-d \to \pi^-\pi^-\pi^+\bar{K}^0np_s$ (Λ and $\bar{K}$ unseen) has been estimated as less than 2% based on the frequency of fit to visible Λ and $\bar{K}$ events. Approximately 60% of the fitted events of both reactions have a permutation ambiguity between K^- and π^- that cannot be removed by X^2 or ionization observation criteria. Whenever possible, a more complicated criterion, which is based on the apparent presence of the well-known resonances such as ρ and $K^*(890)$, was applied to resolve the ambiguity. The procedure is delineated in the next section.

EXPERIMENTAL RESULTS

We estimate the cross section for reaction (1) to be 232 ± 49 μb for visible deuteron events. The total cross section for reaction (1) corrected for unseen deuteron events by a one-pion-exchange (OPE) prediction for $d\sigma/dt(K^- \to K^-\pi^+)$ [$t \leq 0.05$ (GeV/c)^2] was calculated to be 274 ± 56 μb. A similar correction factor was used by Werner *et al.*, who report a corrected total $K^-d \to K^-\pi^-\pi^+d$ cross section of 228 ± 35 μb at 5.5 GeV/c.[13]

The cross section for reaction (2) has been estimated based on three-prong events correcting into the four-prong region via the Hulthén distribution.[14] We estimate the cross section for reaction (2) or more properly $K^-n \to K^-\pi^-\pi^+n(p_s)$ to be 2.17 ± 0.29 mb.

In Fig. 1, two-body mass and corresponding t distributions are shown. Where the $K^- - \pi^-$ ambiguity is present, both fits are plotted weighting each by one-half. In reaction (1), $K^*(890)$, $\rho(765)$, and $D^*(2200)$ are observed. Figure 2 shows the distribution of the scattering angle of the deuteron in the πd center-of-mass system for events in the D^{*+} and D^{*-} regions. The distributions are strong-

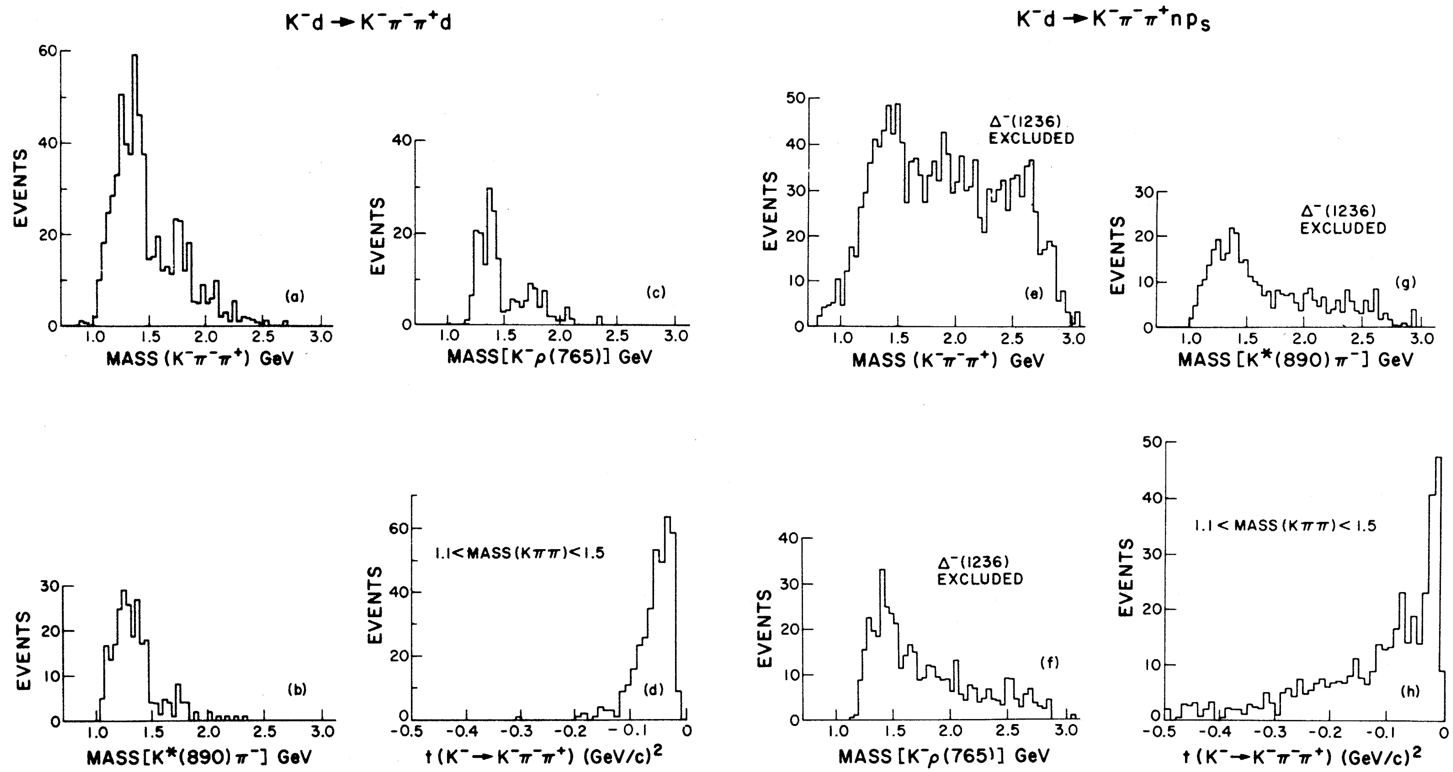

FIG. 3. From $K^-d \to K^-\pi^-\pi^+d$: (a) mass $(K^-\pi^-\pi^+)$, (b) mass $[K^*(890)\pi]$, (c) mass $[K^-\rho(765)]$, and (d) $t(K^- \to K^-\pi^-\pi^+)$ with $1.1 < \text{mass}\ (K^-\pi^-\pi^+) < 1.5$ GeV; and from $K^-d \to K^-\pi^-\pi^+np_s$: (e) mass $(K^-\pi^-\pi^+)$ with $\Delta^-(1236)$ excluded, (f) mass $[K^-\rho(765)]$ with $\Delta^-(1236)$ excluded, (g) mass $[K^*(890)\pi^-]$ with $\Delta^-(1236)$ excluded, and (h) $t(K^- \to K^-\pi^-\pi^+)$ with $1.1 < \text{mass}\ (K^-\pi^-\pi^+) < 1.5$ GeV where, when a $K^-\pi^-$ ambiguity occurred, both fits were plotted weighted by $\frac{1}{2}$.

ly peaked in the forward direction implying the presence of several angular momenta, as observed in previous experiments.[13,15] In reaction (2) production of the resonances $K^*(890)$, $K^*(1420)$, $\rho(765)$, and $\Delta^-(1236)$ is observed with quasi-two-body final states $K^*(890)\Delta^-(1236)$ and $K^*(1420)\Delta^-(1236)$ accounting for approximately 40% of the $\Delta^-(1236)$ production.

In Fig. 3, the $K\pi\pi$ distributions are shown with ambiguous events treated as in Fig. 1.[16] Both reactions show the broad Q enhancement between 1.1 and 1.5 GeV. Evidence of $L(1775)$ production is observed only in reaction (1). It does not appear to be associated with $K_N(1420)$ [not clearly evident in Fig. 1(a)] as has been reported in previous experiments.[17]

Upon close examination one notes that the $\rho(765)$ enhancement in reaction (2) [Fig. 1(j)] is shifted slightly to lower mass values. If we examine the $\pi^-\pi^+$ effective-mass distribution of ambiguous events for which the other fit to the event (with K^- and π^- permuted) gives a $K^-\pi^+$ mass in the $K^*(890)$ band [Fig. 4(a)], we see that the distribution drops off sharply above 800 MeV. $K^*(890)$ events appear to account for at least part of the $\pi^-\pi^+$ enhancement in Fig. 1(j). If a $K^-\pi^+$ mass in the $K^*(890)$ band is used as an additional criterion for selecting the correct fit [Fig. 4(b)], all of the $\pi^-\pi^+$ enhancement below 800 MeV is removed. The remaining enhancement above 800 MeV offers limited evidence that true $\rho(765)$ events were present in the data. The events uniquely determined by ionization [shaded in Fig. 4(b)] also show some evidence of $\rho(765)$. A similar situation is encountered in reaction (1).

This ambiguity complicates any discussion of the $K\pi\pi$ effective-mass distribution since Q production is observed to be associated with $K^*(890)$ and $\rho(765)$. In the examination of the $K\pi\pi$ distributions that follows, this ambiguity has been removed by selecting fits on $K^*(890)$ and $\rho(765)$, selecting in that order. Such a procedure must by its nature cause an overestimate of $K^*(890)$. $K^*(890)$ selection should deplete any true $\rho(765)$ signal and $\rho(765)$ selection should deplete the $\pi\pi$ distribution outside the $\rho(765)$ band. One would not expect incorrectly selected fits to add preferentially to the Q region. Not selecting legitimate $K^*(890)$ and $\rho(765)$ events would however cause a depletion.

The resulting two-body mass and corresponding t distributions are shown in Fig. 5 with selected events shaded. The $K^-\pi^-\pi^+$ mass distributions are shown in Fig. 6. In both reactions the broad Q enhancement from 1.1 to 1.5 GeV is observed. Some evidence of splitting is observed in reaction (1) with resonances at 1250 and a peak around 1400 MeV. In Fig. 7 the $K^*(890)\pi^-$ and $K^-\rho(765)$ mass distributions are shown. In reaction (2) the $K^*(890)\pi^-$ mass distribution shows evidence of splitting of the Q. This splitting is not clearly observed in the $K^*(890)\pi^-$ mass distribution of reaction (1). In both reactions some evidence of splitting in the $K^-\rho(765)$ distributions is observed, although statistics do not allow a definite statement.

OPE-MODEL CALCULATION

One-pion-exchange calculations have been made for reaction (2) using an off-mass-shell correction proposed by Benecke and Durr.[18] The diagrams are shown in Figs. 8(a) and 9(a). Wolf has carried out a series of calculations using this off-shell correction for $\pi p \to 3\pi p$ data from 2.1 to 20 GeV/c.[19] Only distributions involving particles produced at the same vertex were calculated since cross-diagram terms require an accurate knowledge of the elastic scattering phase-shift analysis for each vertex. The model was quite successful in accounting for the general features of the data.

We have made a cross-diagram calculation for the $K^*\pi$ and $K\pi\pi$ distributions. Saclay's πN elastic scattering phase-shift-analysis data were used up to 1560 MeV laboratory kinetic energy of the pion.[20] Above 1560 MeV where no reliable phase-shift data were available, interference in the πN scattering was assumed to be approximately equivalent on and off the mass shell and a polynomial fit to the scattering data was used.[21] The $K\pi_{\text{off}} \to K^*(890)$ coupling was assumed to be proportional to the $\pi\pi_{\text{off}} \to \rho(765)$ value of Wolf, scaled by the ratio of the ρ and K^* widths or lifetimes since the interaction radius should be proportional to interaction time for similar coupling. The model was found to be fairly insensitive to this number.

The calculation was normalized to the $\Delta^-(1236)$

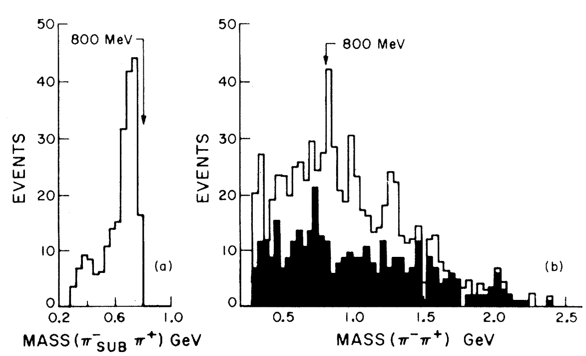

FIG. 4. (a) $\pi^-\pi^+$ effective mass for $K^-\pi^-$ ambiguous events where the $K^-\pi^+$ effective mass of the other fit was in the $K^*(890)$ band. (b) $\pi^-\pi^+$ effective mass where all possible $K^*(890)$ events have been removed, events uniquely determined by ionization are shaded.

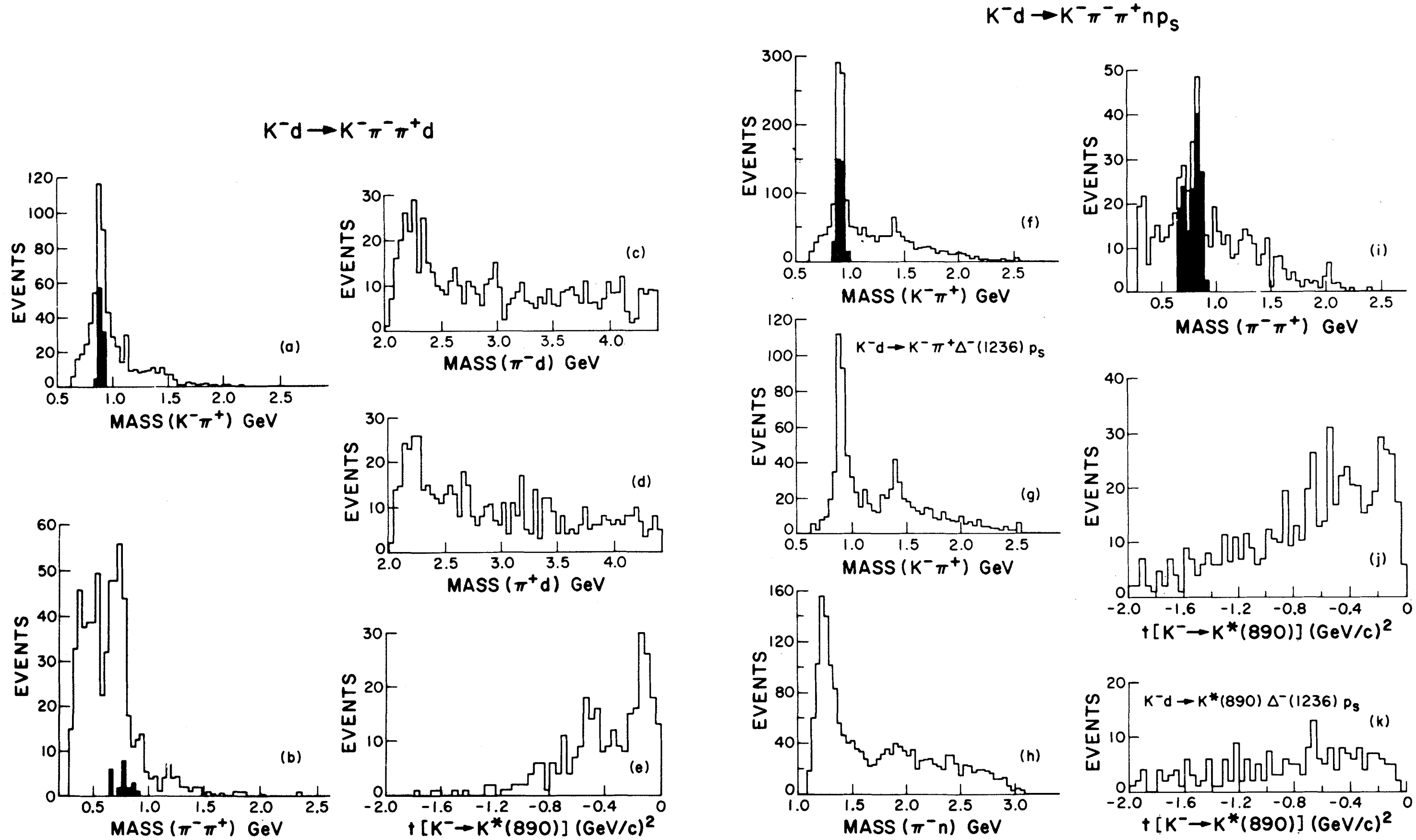

FIG. 5. From $K^-d \rightarrow K^-\pi^-\pi^+d$: (a) mass $(K^-\pi^+)$, (b) mass $(\pi^-\pi^+)$, (c) mass (π^-d), (d) mass (π^+d), and (e) $t(K^- \rightarrow K^*(890))$; and from $K^-d \rightarrow K^-\pi^-\pi^+np_s$: (f) mass $(K^-\pi^+)$, (g) mass $(K^-\pi^+)$ in $K^-\pi^+\Delta^-(1236)_s$, (h) mass (π^-n), (i) mass $(\pi^-\pi^+)$ with $K^*(890)$ and $\Delta^-(1236)$ excluded, (j) $t(K^- \rightarrow K^*(890))$, and (k) $t(K^- \rightarrow K^*(890))$ in $K^*(890)\Delta^-(1236)p_s$. When the $K^-\pi^+$ ambiguity was present, fits were selected on $K^*(890)$ and $\rho(765)$. The events selected are shaded.

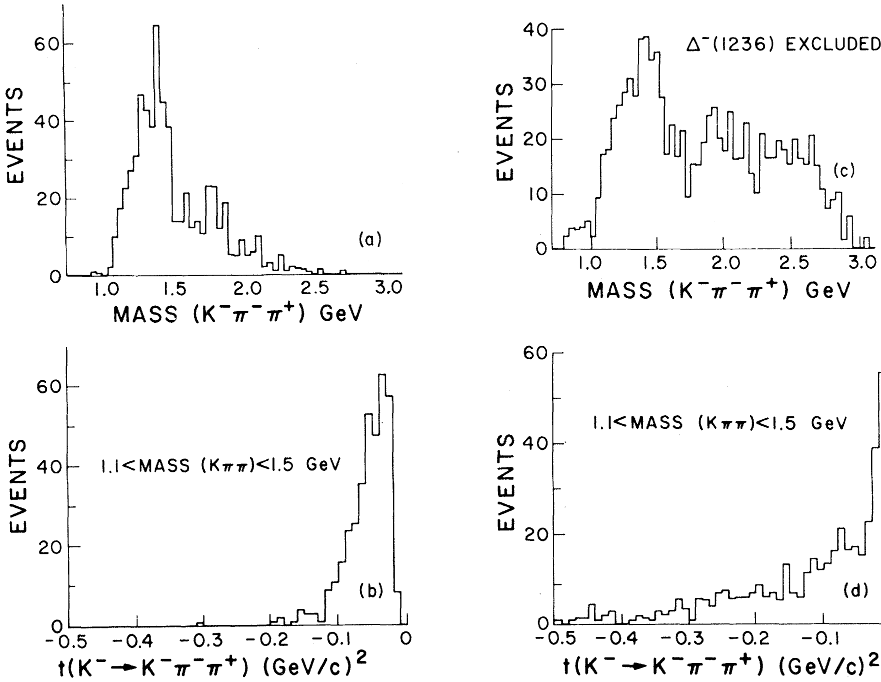

FIG. 6. From $K^-d \to K^-\pi^-\pi^+d$: (a) mass $(K^-\pi^-\pi^+)$ and (b) $t(K^- \to K^-\pi^-\pi^+)$ with $1.1 < \text{mass}\ (K^-\pi^-\pi^+) < 1.5$ GeV; and from $K^-d \to K^-\pi^-\pi^+np_s$: (c) mass $(K^-\pi^-\pi^+)$ with $\Delta^-(1236)$ excluded and (d) $t(K^- \to K^-\pi^-\pi^+)$ with $1.1 < \text{mass}\ (K^-\pi^-\pi^+) < 1.5$ GeV. Events selected on $K^*(890)$ and $\rho(765)$ as in Fig. 5.

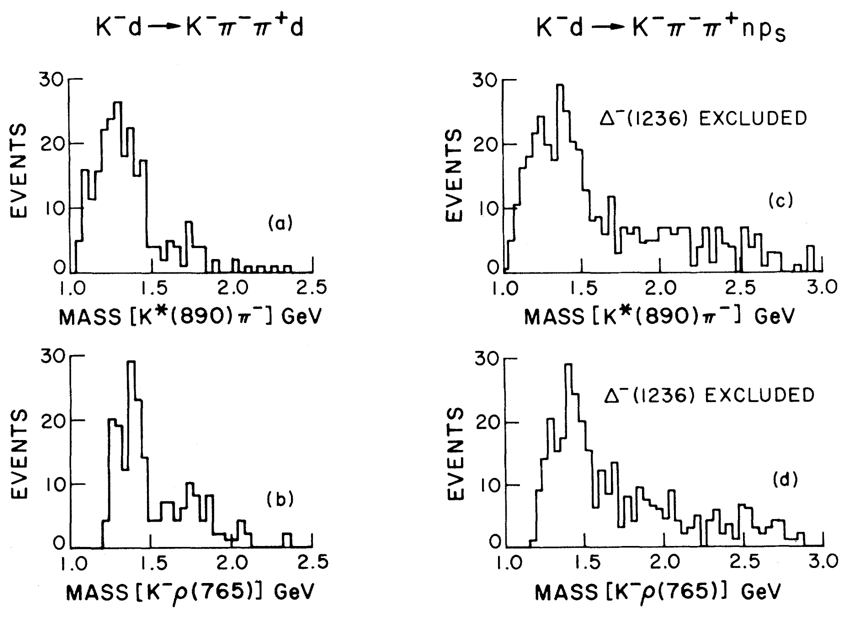

FIG. 7. From $K^-d \to K^-\pi^-\pi^+d$: (a) mass $[K^*(890)\pi]$ and (b) mass $[K^-\rho(765)]$; and from $K^-d \to K^-\pi^-\pi^+np_s$: (c) mass $[K^*(890)\pi^-]$ with $\Delta^-(1236)$ excluded and (d) mass $[K^-\rho(765)]$ with $\Delta^-(1236)$ excluded. Events were selected as in Fig. 5.

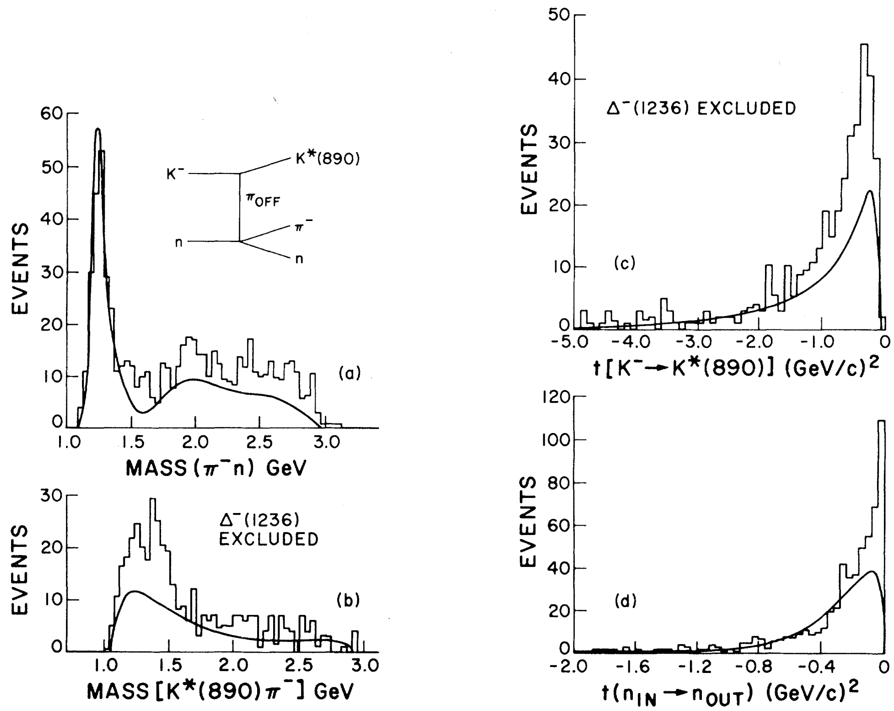

FIG. 8. The OPE calculation and the data for (a) mass ($\pi^- n$), (b) mass [$K^*(890)\pi^-$] with $\Delta^-(1236)$ excluded, (c) $t(K^- \rightarrow K^*(890))$ with $\Delta^-(1236)$ excluded, and (d) $t(n_{in} \rightarrow n_{out})$.

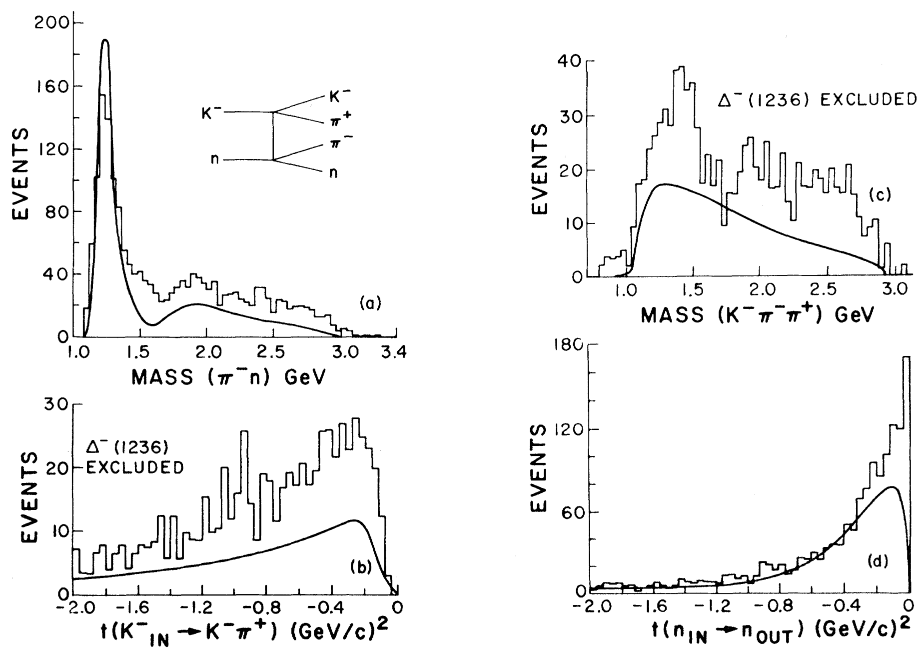

FIG. 9. The OPE calculation and the data for (a) mass ($\pi^- n$), (b) $t(K^- \rightarrow K^-\pi^+)$ with $\Delta^-(1236)$ excluded, (c) mass ($K^-\pi^-\pi^+$) with $\Delta^-(1236)$ excluded, and (d) $t(n_{in} \rightarrow n_{out})$.

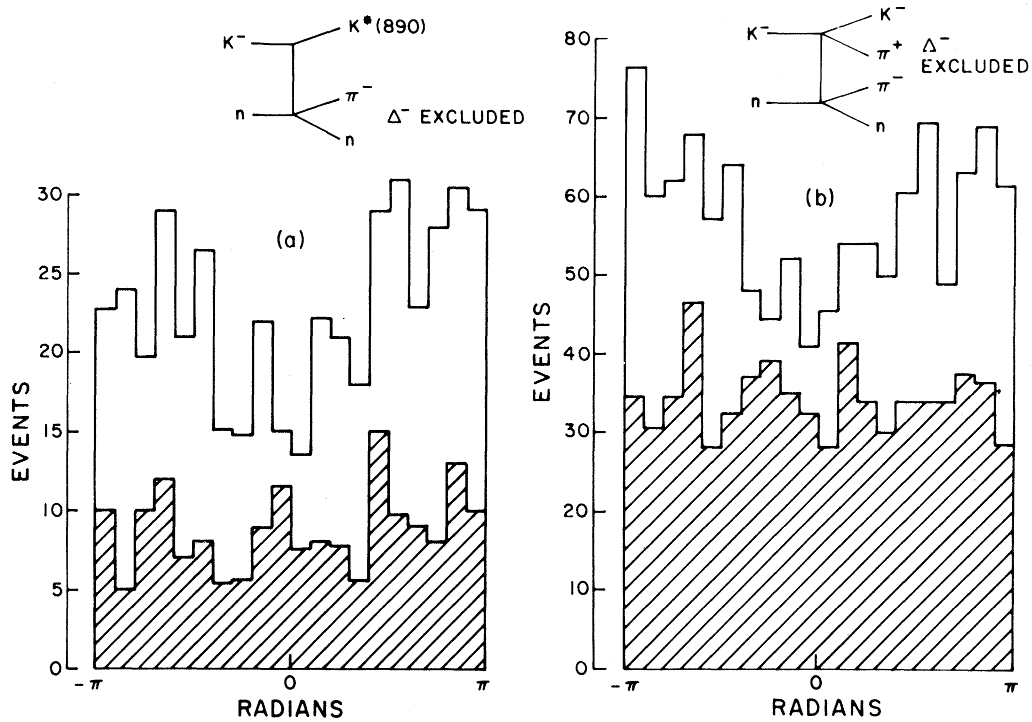

FIG. 10. Treiman-Yang angle distributions for (a) $K^*(890)\pi^-n$ and (b) $K^-\pi^-\pi^+n$. Shaded portions are with the Q region [mass $(K^-\pi^-\pi^+) < 1.6$ GeV] removed.

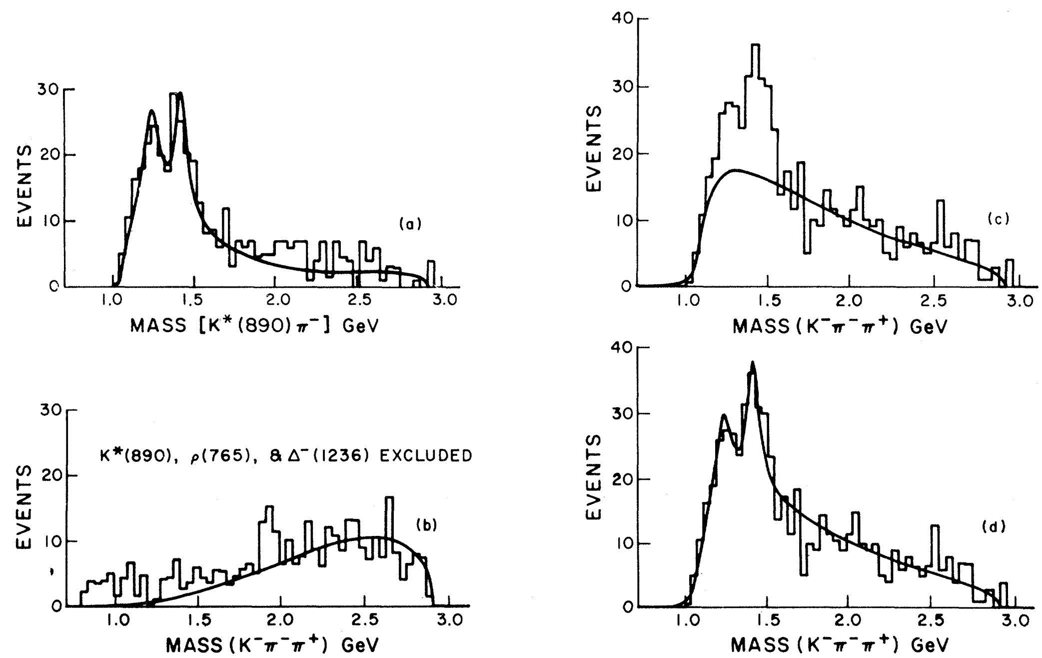

FIG. 11. (a) mass $[K^*(890)\pi]$ and the OPE calculation plus two Breit-Wigner functions fitted to the data; (b) mass $(K^-\pi^-\pi^+)$ with $K^*(890)$, $\rho(765)$, and $\Delta^-(1236)$ excluded and phase space; (c) mass $(K^-\pi^-\pi^+)$ with events in diagram (b) removed and the OPE calculation; (d) OPE plus two Breit-Wigner functions fitted to the data in diagram (c).

region of the data. The results of the calculation for $K^-n \to K^*(890)\pi^-n$ are shown in Fig. 8 with the data. No t cuts have been made in the model or the data. The Q peak cannot be attributed solely to kinematic reflection. The model predicts a peaking of the mass distribution in the Q region but not as strongly as is observed in the data. In addition, the Treiman-Yang angular distribution [Fig. 10(a)] is not flat unless events in the Q region are removed. Two Breit-Wigner functions were added to the model and fitted to the data in Fig. 11(a). The resulting masses and widths were (in MeV) $M_1 = 1228 \pm 21$, $\Gamma_1 = 111 \pm 33$, $M_2 = 1414 \pm 15$, and $\Gamma_2 = 89 \pm 24$ with cross sections 86 ± 11 μb and 90 ± 13 μb, respectively.

The calculation for $K^-n \to K^-\pi^-\pi^+n$ is shown in Fig. 9. $K^-\pi^+$ scattering data (Fig. 12) determined by Urvater in an on-shell calculation for $K^-p \to K^-\pi^-\pi^+p$ were used.[22] They consisted of a peak at the $K^*(890)$ on a smooth background. Using this

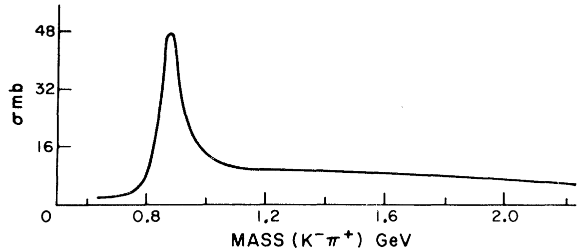

FIG. 12. $K^-\pi^+$ elastic scattering cross section as determined by Urvater in on-shell OPE calculation.

information, the K^* mass was varied in the preceding calculation over the allowed $K^-\pi^+$ effective-mass range and the results at each mass value were weighted by the corresponding $K^-\pi^+$ cross section. Normalization was taken from the previous calculation. The resulting $\Delta^-(1236)$ peak was considerably stronger than in the data and it

TABLE I. Cross sections of the different final states.

Resonance or state	σ (μb)	$\Delta\sigma$ (μb)	Comment
$K^-\pi^-\pi^+d$; visible deuteron	232	± 43	Resonance cross sections based on this number
$K^-\pi^-\pi^+d$; corrected for unseen deuteron by linear extrapolation of $\ln(d\sigma/dt)$	506	± 110	
$K^-\pi^-\pi^+d$; corrected for unseen deuteron by OPE prediction for $d\sigma/dt$, $\lvert t\rvert \le 0.05$ (GeV/c)^2	274	± 56	Simple on-shell OPE with exponential approximation of π^-d scattering
$K^{*0}(890)$	141	± 26	
$D^{*0}(2200)$	66	± 13	No unique spin; see text
$K^{*0}(890)D^{*0}(2200)$	29	± 8	
$\rho(765)$	33	$^{+6}_{-33}$	Observation uncertain; see text
$K^-\pi^-\pi^+np_s$	2170	± 290	Based on invisible-spectator events corrected via Hulthén distribution; see text
$K^{*0}(890)$	836	$^{+143}_{-132}$	
$K^{*0}(890)\Delta^-(1236)$	335	± 33	
$K^{*0}(1420)$	174	± 23	
$K^{*0}(1420)\Delta^-(1236)$	168	± 22	
$\Delta^-(1236)$	1311	$^{+223}_{-275}$	
$\rho(765)$	148	$^{+68}_{-148}$	Observation questionable; see text
$K_A(1250)$	99.2	$^{+60.6}_{-13.4}$	Model-dependent upper limits from Breit-Wigner functions plus OPE fit to $K\pi\pi$ distribution without phase-space-type background subtracted; see text
$K_A(1250) \to K^*(890)\pi$	85.7	± 11	
$K_A(1250) \to K^-\rho(765)$	13.4	$^{+47.2}_{-13.4}$	
$K_A(1400)$	103.8	$^{+49.8}_{-13.9}$	
$K_A(1400) \to K^*(890)\pi^-$	89.9	± 13	
$K_A(1400) \to K^-\rho(765)$	13.9	$^{+35.9}_{-13.9}$	

was necessary to scale up the ratio of $K^*(890)$ to background by 42% to fit the $\Delta^-(1236)$.[23] As before only part of the Q production is predicted by the model and the Treiman-Yang angle distribution [Fig. 10(b)] is flat only after removal of events in the Q region. In addition, the data do not fall off at high mass values as rapidly as the model predicts.

A possible explanation of the high-mass disagreement is the presence of a phase-space-type background. If $K^*(890)$, $\rho(765)$, and $\Delta^-(1236)$ events are removed from the $K\pi\pi$ distribution [Fig. 11(b)], the data have the general shape predicted by phase space. When these events are removed from the $K\pi\pi$ distribution [Fig. 11(c)] the high-mass behavior of the data is consistent with the model. In Fig. 11(d) the smooth curve corresponds to two Breit-Wigner functions added to the model and fitted to the data. The resulting cross sections were 99.2 μb and 103.8 μb, respectively, for the lower and upper peaks. If the difference between this and the $K^*\pi^-$ fits is attributed to $K\rho(765)$ decay, then an upper limit on the branching ratios of 13.5% and 13.9% result for the $K^-\rho(765)$ mode. The $K^-\rho(765)$ mass distribution [Fig. 7(d)] does not appear to be inconsistent with resonance production.

CONCLUSION

Splitting of the Q appears to be a constant feature throughout the data. Although the statistical validity of the evidence is inconclusive, the data do support the hypothesis that the Q consists of two resonances. The cross sections calculated are based on the one-pion-exchange model with the Benecke-Durr off-mass-shell correction as an estimate of Q background. We have made no attempt to determine the presence of $K_N^*(1420)$ in the upper peak. An estimate could be made based on the reaction $K^-d \to \pi^-K^0np_s$, but the unseen neutron makes this a difficult reaction to work with and experiments in hydrogen should give better results.

Resonance production cross sections are summarized in Table I. The $K^-\pi^-$ ambiguity complicates the determination and results in the large uncertainties. This is particularly true of $\rho(765)$, where even the presence of the resonance can be questioned.

Goldhaber has suggested that the Q consists of two interfering resonances with relative phase varying with beam momentum.[24] This could account for the inconsistency in resonance observation found in the Q experiments. Our data appear to be consistent with this interpretation.

---

*Work supported by the U. S. Atomic Energy Commission.

[1]A. Firestone, in *Experimental Meson Spectroscopy*, edited by C. Baltay and A. Rosenfeld (Columbia Univ. Press, New York, 1970), p. 229.

[2]A. Garfinkel *et al.*, Phys. Rev. Letters 26, 1505 (1971).

[3]P. J. Davis *et al.*, Phys. Rev. D 5, 2688 (1972).

[4]R. Armenteros *et al.*, Phys. Letters 9, 207 (1964).

[5]J. Barash *et al.*, Phys. Rev. 145, 1095 (1966).

[6]D. Crennell *et al.*, Phys. Rev. Letters 19, 44 (1967).

[7]A. Astier *et al.*, Nucl. Phys. B10, 65 (1969).

[8]A. Bettini *et al.*, Nuovo Cimento 62A, 1038 (1969).

[9]C. Chien *et al.*, Phys. Letters 28B, 143 (1968).

[10]G. Goldhaber *et al.*, Phys. Rev. Letters 19, 972 (1967).

[11]M. Faber *et al.*, Phys. Rev. D 1, 78 (1970).

[12]F. Bomse *et al.*, Phys. Rev. Letters 20, 1519 (1968).

[13]B. Werner *et al.*, Phys. Rev. 188, 2023 (1969).

[14]B. Erikson *et al.*, Arkiv Fysik 25, 463 (1963).

[15]W. Hoogland *et al.*, Nucl. Phys. B11, 309 (1969).

[16]Throughout we have used 840 MeV $< K^*(890) <$ 940 MeV, 1116 MeV $< \Delta^-(1236) <$ 1356 MeV, and 640 MeV $< \rho(765) <$ 890 MeV for resonance bands in the plots presented.

[17]C. Chien, in *Experimental Meson Spectroscopy*, edited by C. Baltay and A. Rosenfeld (Columbia Univ. Press, New York, 1970), p. 275.

[18]J. Benecke and H. P. Durr, Nuovo Cimento 56A, 269 (1968).

[19]G. Wolf, Phys. Rev. 182, 1538 (1969).

[20]P. Bareyre *et al.*, Phys. Rev. 165, 1730 (1968).

[21]D. M. Alvarado and E. Urvater, University of Colorado Report No. UA-3, 1967 (unpublished).

[22]E. Urvater, Ph.D. thesis, University of Colorado, 1968 (unpublished).

[23]Y. Cho *et al.*, University of Kansas report, 1971 (unpublished). This experiment has found a $K^-\pi^-$ cross-section distribution approximately 50% of that reported by Urvater.

[24]G. Goldhaber, Phys. Rev. Letters 19, 976 (1967).